Wiley
Journal of Food Biochemistry
Volume 2024, Article ID 9994944, 12 pages
https://doi.org/10.1155/jfbc/9994944

WILEY

Research Article

Flavonoids Isolated From *Delphinium semibarbatum* Flowering Aerial Parts With Their Antibacterial, Antibiofilm, and Antiswarming Activity Against *Proteus mirabilis* and *Staphylococcus aureus*

Mohammadreza Lotfaliani,[1] **Seyed Abdulmajid Ayatollahi**,[2,3] **Farzad Kobarfard**,[4] **Mohammad Bagher Majnooni**,[5] **Arezoo Mirzaei**,[6] **Mustafa Ghanadian**,[7] **and Mohammad Hossain Farzaei**[5]

[1]*Department of Pharmacognosy, School of Pharmacy, Shahid Sadoughi University of Medical Science and Health Service, Yazd, Iran*
[2]*Phytochemistry Research Center, Shahid Beheshti University of Medical Science, Tehran, Iran*
[3]*Department of Pharmacognosy, School of Pharmacy, Shahid Beheshti University of Medical Science, Tehran, Iran*
[4]*Department of Medical Chemistry, Phytochemistry Research Center, School of Pharmacy, Shahid Beheshti University of Medical Science, Tehran, Iran*
[5]*Pharmaceutical Sciences Research Center, Health Institute, Kermanshah University of Medical Sciences, Kermanshah, Iran*
[6]*Department of Bacteriology and Virology, Faculty of Medicine, Isfahan University of Medical Science, Isfahan, Iran*
[7]*Department of Pharmacognosy, Isfahan Pharmaceutical Sciences Research Center, School of Pharmacy, Isfahan University of Medical Sciences, Isfahan, Iran*

Correspondence should be addressed to Mustafa Ghanadian; ghannadian@gmail.com and Mohammad Hossain Farzaei; mh.farzaei@gmail.com

Received 30 December 2023; Revised 7 August 2024; Accepted 10 October 2024

Academic Editor: Erick Gutiérrez-Grijalva

Copyright © 2024 Mohammadreza Lotfaliani et al. This is an open access article distributed under the Creative Commons Attribution License, which permits unrestricted use, distribution, and reproduction in any medium, provided the original work is properly cited.

Proteus mirabilis and *Staphylococcus aureus* are pathogens associated with CAUTIs. Understanding their significance is crucial for effective prevention and treatment. In this study, the *Delphinium semibarbatum* flavonoid-rich fraction (DSF) was analyzed, and its antibacterial, antibiofilm, and antiswarming properties against these two bacterial species were evaluated. In the phytochemical analysis, four flavonoids, including kaempferol, 4′-O-methyl quercetin, quercetin, and kaempferol-3-O-beta-D-glucopyranoside (K3G), were isolated. The minimum inhibitory concentration (MIC_{50}) of DSF on *P. mirabilis* and *S. aureus* was 1000 μg/mL. Similarly, kaempferol, K3G, and 4′-O-methyl quercetin exhibited inhibitory effects of 20%, 13%, and 12%, respectively, at a concentration of 1000 μg/mL compared to the *P. mirabilis* control. However, the MIC_{50} of kaempferol and 4′-O-methyl quercetin for *S. aureus* were 125 μg/mL and 62.25 μg/mL, respectively. K3G exhibited an inhibitory effect of 37% at a concentration of 1000 μg/mL. DSF reduced biofilm at 1 mg/mL by 78% and 74% for *P. mirabilis* and *S. aureus*, respectively. Quercetin was the most effective in inhibiting *P. mirabilis* biofilm formation, with a 96% inhibition rate, followed by kaempferol and K3G, with 67% and 29%, respectively, at the same concentration. The best bioactive compound against biofilm inhibition of *S. aureus* was quercetin at 250 μg/mL, exhibiting 90% inhibition, followed by K3G, 4′-O-methyl quercetin, and kaempferol with 81%, 45%, and 33%, respectively, at a concentration of 125 μg/mL. In the swarming inhibition assay, DSF showed 78% inhibition at concentrations of 5 μg/mL. Similarly, all bioactive compounds showed 45% antiswarming activity at this concentration. The docking results of the isolated flavonoids on two target proteins, SarA and MrpH, showed that the presence of the methoxy group in the structure of 4′-O-methyl quercetin reduced its interaction with these two proteins. In the ADMET prediction, isolated flavonoids showed good predicted properties suitable for treating these two microbial species in urinary infection diseases.

1. Introduction

Infections caused by the use of catheters are very important in urinary diseases. *Proteus mirabilis* and *Staphylococcus aureus* are two common pathogens associated with CAUTIs, and understanding their significance is crucial for effective prevention, diagnosis, and treatment. *P. mirabilis* is a Gram-negative bacterium known for its motility, biofilm formation, and production of urease, which can cause obstruction and persistent infection, especially in subjects with longer catheterization periods [1]. *S. aureus*, a Gram-positive bacterium, possesses virulence factors that enable it to form biofilms on catheters, leading to severe complications [2]. Biofilm increases drug resistance and reduces the immune system's effectiveness [3]. These infections contribute to increased morbidity, longer hospital stays, and higher costs, particularly with the emergence of antibiotic-resistant strains like MRSA [4]. The discovery of new lead compounds against *P. mirabilis* and *S. aureus* in CAUTIs is vital for implementing appropriate prevention and treatment strategies and minimizing their impact on patients and healthcare systems. While conventional medical treatments are the standard approach for managing CAUTIs, the use of complementary and alternative therapies, such as phytotherapy or herbal medicine, has gained attention as a potential adjunctive treatment strategy. Delphinium species are among the medicinal plants studied for antibacterial effects [5–7]. For example, in a study on different extracts of *D. cashmerianum*, its ethyl acetate extract showed the best antibacterial activity against *Streptococcus pneumoniae* and *Klebsiella pneumoniae* with a MIC of 6.3 and 25.0 μg/mL, respectively [5]. In another research, *D. denudatum* ethanol stem extract and aqueous leaf extract showed antimicrobial activity against *Serratia marcescens* and *Nocardia tenirefensis* [6]. In a different study, among different plant species, *D. speciosum* hexane extract and its fractions showed higher antibacterial properties [7]. Delphinium from the Ranunculaceae family contains mainly diterpene alkaloids and flavonoids [8]. They have limited application as herbal medicines to treat inflammatory disorders such as jaundice, rheumatism, toothache, and neuralgia [8]. *D. semibarbatum* (yellow larkspur) from the northeast part of Iran was previously reported as *D. zalil*, but it was introduced as a new species recently [9]. In previous research by the same team on this plant, proapoptotic and cytotoxic effects of its alkaloid extract against prostate cancer lines were reported [10]. This study aims to identify the flavonoid content of *D. semibarbatum*, as well as its antibacterial, antibiofilm, and antiswarming properties, and inhibition of quorum sensing (QS) gene expression of *P. mirabilis* and *S. aureus* strains, in continuation of our previous research in this field [11, 12].

2. Materials and Methods

2.1. General Experimental Procedures. The NMR spectra were done all by a 400 MHz Bruker system using DMSO-d6 as solvent. Silica gel chromatography materials were prepared from Merk, polyamide from Roth in Germany, and Sephadex from Uppsala in Sweden. For flavonoid detection, we employed a Natural product reagent containing 1% 2-aminoethyl diphenylborinate (Merck, Germany) and cerium sulfate reagent containing 1% ceric sulfate (Merck, Germany) solution in 10% sulfuric acid (Mojalali, Iran). The University Ethics Committee approved the study no: IR.SBMU.PHNM.1396.8.

2.2. Plant Material. *D. semibarbatum*, locally known as the yellowish *zaban-dar-ghafa*, was collected from the northeast of Iran, near Sarakhs County. Dr. Joharchi, a botanist from Ferdowsi University of Mashhad, identified it with the number SAM-3392, and it is now preserved in the herbarium of Isfahan University of Medical Sciences.

2.3. Extraction and Isolation. The plant material was air-dried at room temperature and then powdered. After extracting the total alcoholic extract to remove oils and nonpolar compounds, we performed the first extraction using hexane solvent, followed by ethyl acetate. The *D. semibarbatum* ethyl acetate extract (DSEAE, 25 g) was loaded onto a polyamide column (SC6, 22 × 2 cm) using a chloroform: methanol gradient (F1, 100:0; F2, 95:5; F3, 9:1; F4, 8:20, each 400 mL). Notably, F2, as the minor fraction, exhibited a positive reaction to Dragendorff's reagent, which is specific for alkaloids. F3, exhibiting a yellow color upon treatment with the natural product reagent (specific for flavonoids), was selected as the *D. semibarbatum* flavonoid-rich fraction (DSF, 3.5 g). DSF was loaded onto polyamide again, and eluted using chloroform: methanol (F1, 100:0; F2, 98:2; F3, 96:4; F4, 94:6; F5, 92:8; F6, 90:10; F7, 80:20, each 200 mL). Major fractions F5, F6, and F7 were chromatographed separately on the Sephadex LH column (80 × 2 cm) using chloroform: methanol (1:1) as the solvent, yielding flavonoids **1**–**4** in their pure state. We determined the isolated compounds based on their NMR and mass spectra, which agreed with the reported data in the literature. Due to its low quantity, the alkaloid fraction was set aside for further research.

2.4. Antibacterial, Antibiofilm, and Antiswarming Activities

2.4.1. Microbial Culture Media. *P. mirabilis* (ATCC 7002) and *S. aureus* (ATCC) were obtained from the Pasteur Institute of Iran strain bank. *P. mirabilis* was cultured on MacConkey agar, Eosin methylene blue, and blood agar, while *S. aureus* was cultured on LB agar and Mueller–Hinton agar (MHA). The pure colonies were stored in TSB–glycerol (20%) at −20°C for further investigations.

2.4.2. Antibacterial Activities. As described before [12], using the agar well diffusion method, bacterial suspensions were diluted to an OD600 of 0.2 and spread evenly on plates. After creating 6 mm diameter wells, 50 μL of DSF and bioactive compounds in varying concentrations of 62.5 to

1000 μg/mL were added and incubated at 37°C for 24 h. The inhibition diameter around each well was then determined. Ofloxacin (5 μg) and gentamicin (10 μg) discs were used as positive controls, and PBS alone was used as the negative control.

The minimum inhibitory concentration (MIC) values were determined using the broth microdilution method on 96-well microplates as described before, with two-fold serial dilutions of bioactive compounds from 1000 to 62.5 μg/mL [12]. Briefly, using LB broth inoculum of strains with a turbidity of 0.5 McFarland, 1/1000 dilutions were made to a final turbidity of about 5.0×10^4 CFU/mL. 100 μL of samples plus 5 μL of bacterial inoculum was added to each well and incubated at 37°C. After 24 h, plates were read at 595 nm using a microplate reader. The results were reported as MIC_{50}, representing the minimum concentration necessary to inhibit 50% bacterial growth. The positive control was the bacteria and medium, and the negative control was just the medium [13].

$$\%\ \text{antibacterial activities} = \frac{(\text{OD positive control} - \text{OD tested compounds})}{(\text{OD positive control})} \times 100. \quad (1)$$

2.4.3. Antibiofilm Activities. The antibiofilm activity was assessed using a modified crystal violet assay on 96-well plates as previously described [11]. Briefly, 100 μL of each isolate culture was incubated in a 96-well plate for 72 h at 37°C. After removing the media, the biofilms were washed with PBS (pH 7.2) and treated individually with two-fold serial dilutions of samples ranging from 1000 to 62.5 μg/mL. After 48 h of incubation at 37°C, the wells were washed with PBS, fixed with ethanol, dried for half an hour, and stained with 0.1% crystal violet. The wells were then washed with water to remove excess stain, and the OD was read at 590 nm using a microplate reader to calculate $MIBC_{50}$ as follows:

$$\%\ \text{antibiofilm activities} = \frac{(\text{OD positive control} - \text{OD tested compounds})}{(\text{OD positive control})} \times 100. \quad (2)$$

2.4.4. Antiswarming Activities. To evaluate the antiswarming effects, 50 μL of each of the DSF or isolated flavonoids at various concentrations of 62.25, 125, 250, 500, and 1000 μg/mL was added to MHA (10 mL) to reach the final concentration of 0.3125, 0.625, 1.25, 2.5, and 5 μg/mL and poured on the Petri dishes to solidify. Then, 10 μL of overnight incubated cultures of *P. mirabilis* was dropped into the center of the solidified mediums and incubated at 37°C for 3 days, and the areas of the colonies were measured to determine the inhibition of swarming activities [11, 14].

2.5. Molecular Docking. Crystalline structures of *Proteus mirabilis* MrpH (PDB ID: 6Y4E) and *Staphylococcus aureus* SarA (PDB ID: 2FNP) were obtained from the RCSB PDB site (https://www.rcsb.org/structure/6Y4E and https://www.rcsb.org/structure/2FNP). As reported before [15], by Autodock tools version 1.5.6, H_2O, ligands, and cofactors were eliminated, and polar protons were added. The structures of the ligands, including kaempferol, quercetin, 4′-O-methyl quercetin, and kaempferol-3-O-beta-D-glucoside (K3G), were generated by ChemScketch, and energy minimization was done by Chimera software [16]. Molecular docking calculations were done through Autodock Vina in PyRx 0.8 [17] with grid box dimensions (Angstrom) of $X = 22.7269$, $Y = 22.7454$, and $Z = 27.4354$ for MrpH and $X = 33.1255$, $Y = 29.0704$, and $Z = 33.5647$ for SarA, and protein–ligand interactions were illustrated by LigPlot+ [18].

2.6. In Silico ADMET Studies. To evaluate the physicochemical and pharmacokinetics properties of the ligands including the absorption, distribution, and elimination of bioactive compounds, the ADMET application from the SwissADME server (https://www.swissadme.ch) [19] was used. Safety and possible toxic effects were conducted by admetSAR from the https://lmmd.ecust.edu.cn/admetsar1 site [20].

2.7. Statistical Analyses. We did the statistical analysis by prism software through one-way analysis of variance (ANOVA) and Dunnett's post-hoc test taking p value less than 0.05 significant.

3. Results and Discussion

3.1. Identification of the Isolated Compounds. *D. semibarbatum* is used by local people to dye hand-woven carpet threads yellow, likely due to its high flavonoid content. In this study, four flavonol derivatives were isolated as major components (Figure 1) and investigated for their antibacterial activities. Compounds **1**–**4** were obtained in the form of yellowish amorphous powder, showing a positive reaction (deep yellow color) to 1% 2-aminoethyl diphenylborinate, a natural product reagent for flavonoids.

Compound **1**, with m/z mass molecular ion at 287 $[M + H]^+$, and ^{1}H-NMR signals in the downfield area at δ_H 12.49 (s, 1H, 5-OH), 10.82 (s, 1H, 7-OH), 10.16 (s, 1H, 4′-

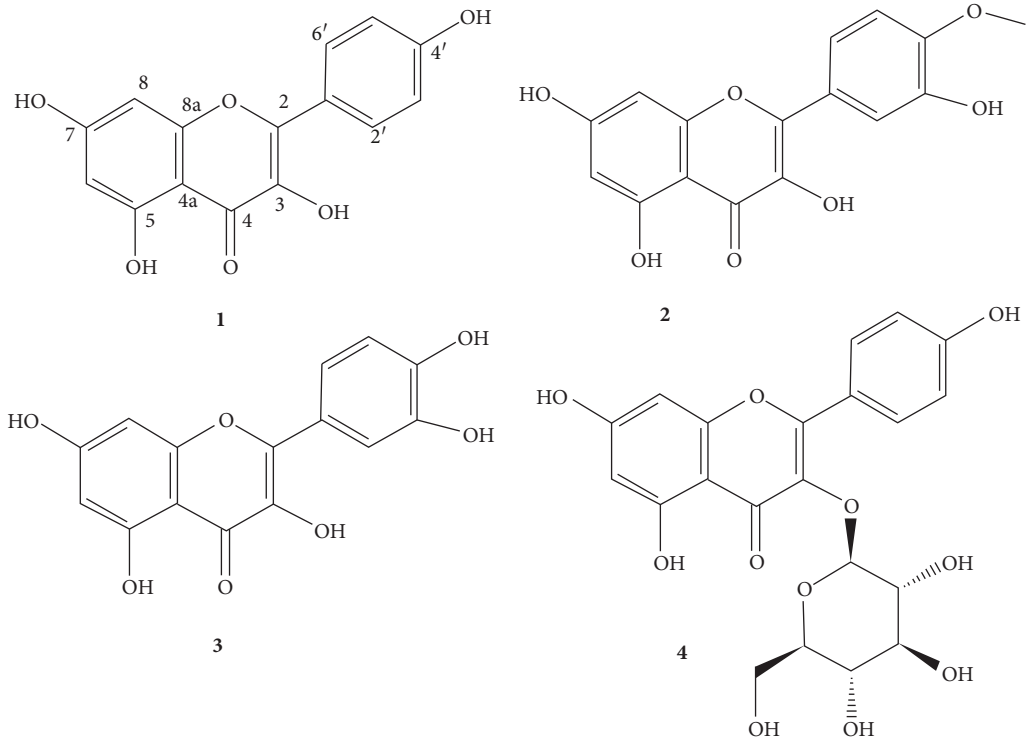

Figure 1: Major flavonoids isolated from the *D. semibarbatum* flavonoid-rich fraction (DSF). DSF contained kaempferol (**1**), 4′-O-methyl quercetin (**2**), quercetin (**3**), and kaempferol-3-O-beta-D-glucoside (**4**).

OH), and 9.43 (s, 1H, 3-OH) related to four phenolic OH groups, as well as four signals at aromatic region at δ_H 8.05 (d, $J = 8.9$, 2H, H2′, 6′), 6.93 (d, $J = 8.9$, 2H, H3′, 5′), 6.45 (d, $J = 2.1$, H8), and 6.20 (d, $J = 2.1$, 1H, H6), was similar to kaempferol data in literature [21]. ^{1}H-NMR spectra of compound **2** showed four phenolic OH resonances in downfield at δ_H 12.47 (s, 1H), 10.81 (s, 1H), 9.76 (s, 1H), and 9.45 (s, 1H), three protons with ABX spin system at δ_H 7.75 (d, $J = 2.1$, 1H, H2′), 7.69 (dd, $J = 8.5$, 2.1, 1H, H6′), and 6.94 (d, $J = 8.5$, 1H, H5′) (H-2′ and H-6′ were *meta*-coupled with $J = 2.1$, and H-6′ and H-5′ *ortho*-coupled with $J = 8.5$), together with two *meta*-coupled doublet protons at 6.48 (d, $J = 2.1$, 1H) and 6.19 (d, $J = 2.1$, 1H) referred to H-8 and H-6, and a methoxy group at δ_H 3.84 (δ_H 3H, s, 3H). Except for methoxy groups, ^{13}C-NMR resonances contained 15 signals at δ_C 93.93 (C8), 98.72 (C6), 103.64 (C4a), 112.42 (C5′), 115.14 (C2′), 120.28 (C6′), 123.92 (C1′), 136.68 (C3), 146.71 (C3′), 146.84 (C2), 149.90 (C4′), 156.69 (C8a), 161.32 (C5), 164.51 (C7), and 176.50 (C4) similar to quercetin analogs. HMBC correlations determined the methoxy group (δ_H 3.84) at 149.90 (C4′). ESI mass showed molecular ions (m/z) at 317 $[M + H]^{+\cdot}$ and 286 $[M\text{-}OCH3]^+$ in agreement with $C_{16}H_{13}O_7$ molecular formula according to NMR data, and finally, it was identified as 4′-O-methyl quercetin [22]. Compound **3** showed a mass (m/z) of 303 $[M + H]^+$ and ^{1}H-NMR data at 12.5 (bs), 10.88 (bs), and 9.15–9.94 (m, 3H) related to 5-OH, 7-OH, and 3, 3′, 4′-OH; 7.67 (d, $J = 2.20$, 1H), 7.54 (dd, $J = 8.5$, 2.20, 1H), and 6.89 (d, $J = 8.5$, 1H) related to H-2′, H-6′, and H5′; 6.42 (d, $J = 2.0$, 1H) and 6.19 (d, $J = 2.0$, 1H) related to H8 and H6. It was similar to **2** but without the methoxy group, and in agreement with quercetin data in the literature [22]. Compound **4** was obtained in the form of a yellowish amorphous powder (21 mg) with a positive reaction (deep yellow color) to the natural product reagent of flavonoids. The ^{1}H-NMR resonances showed typical flavonoid glycoside resonances with two downfield peaks at δ_H 12.64 (s, 1H) and 10.00–10.96 (bs, 2H), for three phenolic OH protons, δ_H 8.03 (d, 2H) and 6.89 (d, 2H) of AA′XX′ ortho coupled spin system ($J = 8.8$) related to H2′, H6′, and H3′, H5′ in ring B, δ_H 6.45, and 6.22 of two meta-coupled ($J = 2.1$) protons in ring A, and δ_H 5.48 (d, $J = 7.30$, H1″) of a beta oriented anomeric signal together with δ_H 4.30–3.10 (m, 6H) of overlapped glycosidic protons (H2″-H6″). ^{13}C-NMR signals at 100.85 (C1″), 74.19 (C2″), 77.49 (C3″), 69.83 (C4″), 76.40 (C5″), and 60.73 (C6″) determined pyranoglucoside attachment [23]. Despite from glycosyl part, remained 15 carbon resonances at 156.35 (C2), 133.50 (C3), 177.44 (C4), 161.17 (C5), 98.68 (C6), 164.15 (C7), 93.64 (C8), 159.97 (C9), 103.97 (C10), 120.83 (C1′), 130.86 (C2′), 115.10 (C3′), 156.22 (C4′), 115.10 (C5′), and 130.86 (C6′) were analogous to those reported for compound 1. ESI ion m/z peak at 449 $[M + H]^+$ as well as NMR data supported molecular formula of $C_{21}H_{20}O_{11}$. Based on these data, compound **4** was elucidated as K3G [23].

3.2. NMR Analysis Data. Kaempferol (**1**). Yellowish white powder; ^{1}H NMR (400 MHz, methyl sulfoxide-d6) δ 12.49 (s, 1H, 5-OH), 10.82 (s, 1H, 7-OH), 10.16 (s, 1H, 4′-OH), 9.43 (s, 1H, 3-OH), 8.05 (d, $J = 8.9$, 2H, H2′, 6′), 6.93 (d,

$J = 8.9$, 2H, H3′, 5′), 6.45 (d, $J = 2.10$, H8), and 6.20 (d, $J = 2.1$, 1H, H6); ^{13}C NMR (100 MHz, methyl sulfoxide-d6): δ 147.11 (C2), 136.33 (C3), 176.40 (C4), 103.29 (C4a), 161.09 (C5), 98.84 (C6), 165.03 (C7), 94.01 (C8), 156.68 (C8a), 122.18 (C1′), 129.87 (C2′, 6′), 115.90 (C3′, 5′), and 159.58 (C4′) [21].

4′-O-Methyl quercetin (**2**). Yellowish white powder; ^{1}H NMR (400 MHz, methyl sulfoxide-d6) δ 12.47 (bs, 1H, 5-OH), 10.81 (bs, 1H, 7-OH), 9.76 (bs, 1H, 3-OH), 9.45 (bs, 1H, 3′-OH), 7.75 (d, $J = 2.1$, 1H, H2′), 7.69 (dd, $J = 8.50$, 2.1, 1H, H 6′), 6.94 (d, $J = 8.50$, 1H, H 5′), 6.48 (d, $J = 2.1$, 1H, H8), 6.19 (d, $J = 2.1$, 1H, H8), and 3.84 (3H, s, 3H, 4′-OCH_3). ^{13}C NMR (100 MHz, methyl sulfoxide-d6): δ_C 56.11 (4′-OCH_3), 93.93 (C8), 98.72 (C6), 103.64 (C4a), 112.42 (C5′), 115.14 (C2′), 120.28 (C6′), 123.92 (C1′), 136.68 (C3), 146.71 (C3′), 146.84 (C2), 149.90 (C4′), 156.69 (C8a), 161.32 (C5), 164.51 (C7), and 176.50 (C4) [22].

Quercetin (**3**). Yellowish white powder; ^{1}H NMR (400 MHz, methyl sulfoxide-d6): δ 12.50 (s, 1H, 5-OH), 10.88 (s, 1H, 7-OH), 9.15–9.94 (3H, 3-OH, 3′-OH, 4′-OH), 7.67 (d, $J = 2.2$, 1H, H2′), 7.54 (dd, $J = 8.5$, 2.2, 1H, H6′), 6.89 (d, $J = 8.50$, 1H, H 5′), 6.42 (d, $J = 2.00$, 1H, H 8), and 6.19 (d, $J = 2.0$, 1H, H6); ^{13}C NMR (100 MHz, methyl sulfoxide-d6): δ 146.81 (C2), 135.83 (C3), 175.89 (C4), 102.04 (C4a), 160.79 (C5), 98.32 (C6), 164.21 (C7), 93.40 (C8), 156.19 (C8a), 122.03 (C1′), 115.09 (C2′), 145.08 (C3′), 147.78 (C4′), 115.72 (C5′), and 120.03 (C6′) [22].

K3G (**4**). Yellowish white powder. ^{1}H NMR (400 MHz, methyl sulfoxide-d6) δ 12.64 (s, 1H, 5-OH), 10.00–10.96 (2H, 7-OH, 4′-OH), 8.03 (d, $J = 8.8$, 2H, H2′, H6′), 6.89 (d, $J = 8.8$, 2H, H3′, H5′), 6.45 (d, $J = 2.1$, 1H, H8), 6.22 (d, $J = 2.1$, 1H, H6), 5.48 (d, $J = 7.3$, 1H, H1″), and 4.30–3.10 (m, H2″-H6″). ^{13}C NMR (100 MHz, methyl sulfoxide-d6): 156.35 (C2), 133.50 (C3), 177.44 (C4), 161.17 (C5), 98.68 (C6), 164.15 (C7), 93.64 (C8), 159.97 (C9), 103.97 (C10), 120.83 (C1′), 130.86 (C2′), 115.10 (C3′), 156.22 (C4′), 115.10 (C5′), 130.86 (C6′), 100.85 (C1″), 74.19 (C2″), 77.49 (C3″), 69.83 (C4″), 76.40 (C 5″), and 60.73 (C 6″) [23].

3.3. Antibacterial, Antibiofilm, and Antiswarming Activities. During a 24-h incubation period, no bactericidal effects against *P. mirabilis* and *S. aureus* were observed with agar well diffusion, regardless of the concentration of DSF or bioactive compounds, including kaempferol (**1**), 4′-O-methyl quercetin (**2**), quercetin (**3**), and K3G (**4**). The MIC_{50} of DSF on *P. mirabilis* and *S. aureus* was 1 mg/mL. Similarly, kaempferol, K3G, and 4′-O-methyl quercetin exhibited inhibitory effects of 20%, 13%, and 12%, respectively, at a concentration of 1 mg/mL compared to the *P. mirabilis* control. However, the MIC_{50} of kaempferol and 4′-O-methyl quercetin for *S. aureus* were 125 μg/mL and 62.25 μg/mL, respectively. K3G exhibited an inhibitory effect of 37% at 500 μg/mL.

In the biofilm formation assay, both DSF and bioactive compounds, including quercetin, 4′-O-methyl quercetin, kaempferol, and K3G, inhibited biofilm formation in a concentration-dependent manner. The optimal concentration of DSF for *P. mirabilis* and *S. aureus* was 1 mg/mL, exhibiting 78% and 74% inhibition, respectively. Among the bioactive compounds, quercetin was the most effective in inhibiting *P. mirabilis* biofilm formation, with a 96% inhibition rate, followed by kaempferol and K3G, which demonstrated inhibition rates of 67% and 29%, respectively, at a concentration of 1000 μg/mL. The best bioactive compound against biofilm inhibition of *S. aureus* was quercetin at 250 μg/mL, exhibiting 90% inhibition, followed by K3G, 4′-O-methyl quercetin, and kaempferol, which showed inhibition rates of 81%, 45%, and 33%, respectively, at 125 μg/mL.

In the swarming inhibition assay, DSF and the identified bioactive compounds exhibited varying degrees of antiswarming effects on *P. mirabilis*, as evidenced by the percentage of inhibition observed. DSF showed 78% inhibition at concentrations of 125–1000 μg/mL, but at a concentration of 62.25 μg/mL, the inhibition decreased to 60%. Similarly, all bioactive compounds showed 45% antiswarming activity at 1000 μg/mL.

Flavonoids are the most extensively studied class of polyphenolic compounds for their pharmacological properties, including antibacterial activity [24], as observed in the present investigation. Previous studies by He et al. and Li et al. have demonstrated that the flavonoids kaempferol 3-O-β-(2‴-acetyl) galactopyranoside and quercetin exert antibacterial effects through the disruption of the cell membrane, followed by the activation of apoptosis and DNA fragmentation. Additionally, kaempferol was found to be the most effective flavonoid tested in damaging the cell membrane of *Escherichia coli*, as evidenced by the observed leakage of bacterial proteins into the extracellular environment, a finding that may be related to the antimicrobial effects observed in the current study [25, 26]. Furthermore, the results of the study by Al-Nour et al. have shown that kaempferol and quercetin interact with 3-oxoacyl-(acyl carrier protein) reductase (FabG) and enoyl-acyl carrier protein reductase, thereby inhibiting the biosynthesis of fatty acids in *Mycobacterium*, *Pseudomonas aeruginosa*, and *Vibrio cholerae*, thus compromising the function of the cell envelope and impeding the formation of bacterial biofilms [27]. In contrast, DSF did not exhibit a bactericidal effect, which is consistent with other studies [11, 12] that have reported alternative aspects of the bioactive compounds' effects on bacteria, including QS inhibition, biofilm disruption, and adhesion inhibition.

The differential effects of bioactive compounds could be attributed to the variations in the cell wall structures between Gram-positive (*S. aureus*) and Gram-negative (*P. mirabilis*) bacteria (Figure 2).

3.4. Molecular Docking Results

3.4.1. Validation of Docking Protocol. To evaluate the accuracy of docking, the ligand (tartaric acid) in the MrpH protein (PDB ID: 6Y4E) was docked in the binding site. The overlap of these two conformations of tartaric acid is shown in Figure 3. The calculated RMSD was 0.57 Å. Typically, an RMSD of less than 2 Å is considered acceptable and suggests the accuracy of the docking methodology [17].

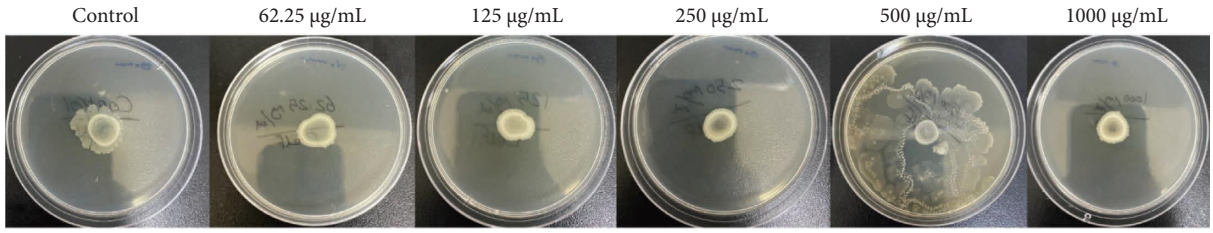

Figure 2: Antiswarming activities of *Delphinium semibarbatum* flavonoid-rich fraction (DSF) against *P. mirabilis*.

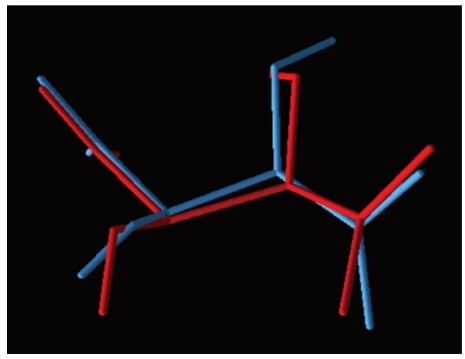

Figure 3: Superposition of cocrystallized ligand (tartaric acid): blue (in MrpH protein, PDB ID: 6Y4E); redocked ligand: red.

3.4.2. Molecular Docking With MrpH. The mannose-resistant Proteus-like (MR/P) fimbriae, which function as adhesion factors for the opportunistic pathogen *P. mirabilis*, are hypothesized to play a pivotal role in facilitating biofilm formation. This is likely achieved through the fimbriae mediating attachment to surfaces and promoting autoaggregation of the bacterial cells [28]. The binding affinity values for all four compounds were almost similar, as shown in Table 1. Kaempferol, with a binding affinity (BA) of −5.7 kcal per mol, was docked in MrpH. One hydrogen bond (H-bond) was found between O4 in the hydroxy function and Asn82 with a bond size of 2.83 Å, and three hydrophobic interactions were formed with the key residues, including Ile140, Arg118, and Thr116 (Figure 4(a)).

4′-O-methyl quercetin established a BA of −6.1 kcal per mol and, through O5 in the hydroxy function, interacted by two H-bonds with residues of Thr116 and Arg118 (bond size: 2.96 and 3.24 A°, respectively) (Figure 4(b)). It also interacted with Asn82 by hydrophobic interaction.

Quercetin showed a BA of −6.0 kcal per mol. One H-bond was found between O4 in the hydroxy function and Arg118 (bond size: 3.11 A°). This compound through hydrophobic interactions correlated with Thr116, His117, and Asn82 (Figure 4(c)).

K3G showed a BA of −5.9 kcal per mol. Three H-bonds were formed between O5, O7, and O10 in the hydroxy functions and Thr116 (bond sizes: 3.17, 2.99, and 2.72 Å, respectively) (Figure 4(d)). Additionally, one H-bond was formed between O11 in the hydroxyl group and Arg118 (bond size: 2.95 Å). Ile140, Asn82, and His72 were also involved in these interactions hydrophobically. These results suggest that molecular docking simulation showed these flavonoids were stably bound to the active site of MrpH and indicated their potential in antibiofilm development and swarming motility inhibition in *P. mirabilis*.

Table 1: Docking results of the ligands with MrpH and SarA.

	Binding affinity (kcal/mol)
Ligand	MrpH and SarA
Kaempferol	−5.7–7.2
4′-O-methyl quercetin	−6.1–6.8
Quercetin	−6.0–7.4
Kaempferol-3-O-beta-D-glucoside (K3G)	−5.9–7.4

As such, the identification and examination of these flavonoids capable of inhibiting MrpH as one of the virulence mechanisms may present a promising alternative therapeutic approach for mitigating infections caused by *P. mirabilis* [29]. These results are in agreement with Majnooni and coworkers on flavonoids isolated from *Allium colchicifolium* leaves. In that study, flavonoids bound to the active site similarly through hydrogen and hydrophobic bonds and with BA values of −5.50, −5.50, −5.70, −5.80, and −6.20 for isorhamnetin, morin, quercetin, isorhamnetin-3-O-glucoside, and quercetin 3-O-glucoside, respectively [12].

3.4.3. Molecular Docking With SarA. *S. aureus*, a prevalent opportunistic pathogen, possesses a complex regulatory network that orchestrates the synthesis of an array of virulence factors [30]. One such regulatory system is the staphylococcal accessory regulator (sarA), which has been demonstrated to enhance biofilm formation in this species [31]. In this study, kaempferol, with a binding affinity (BA) of −7.2 kcal/mol, was docked into the binding site of SarA

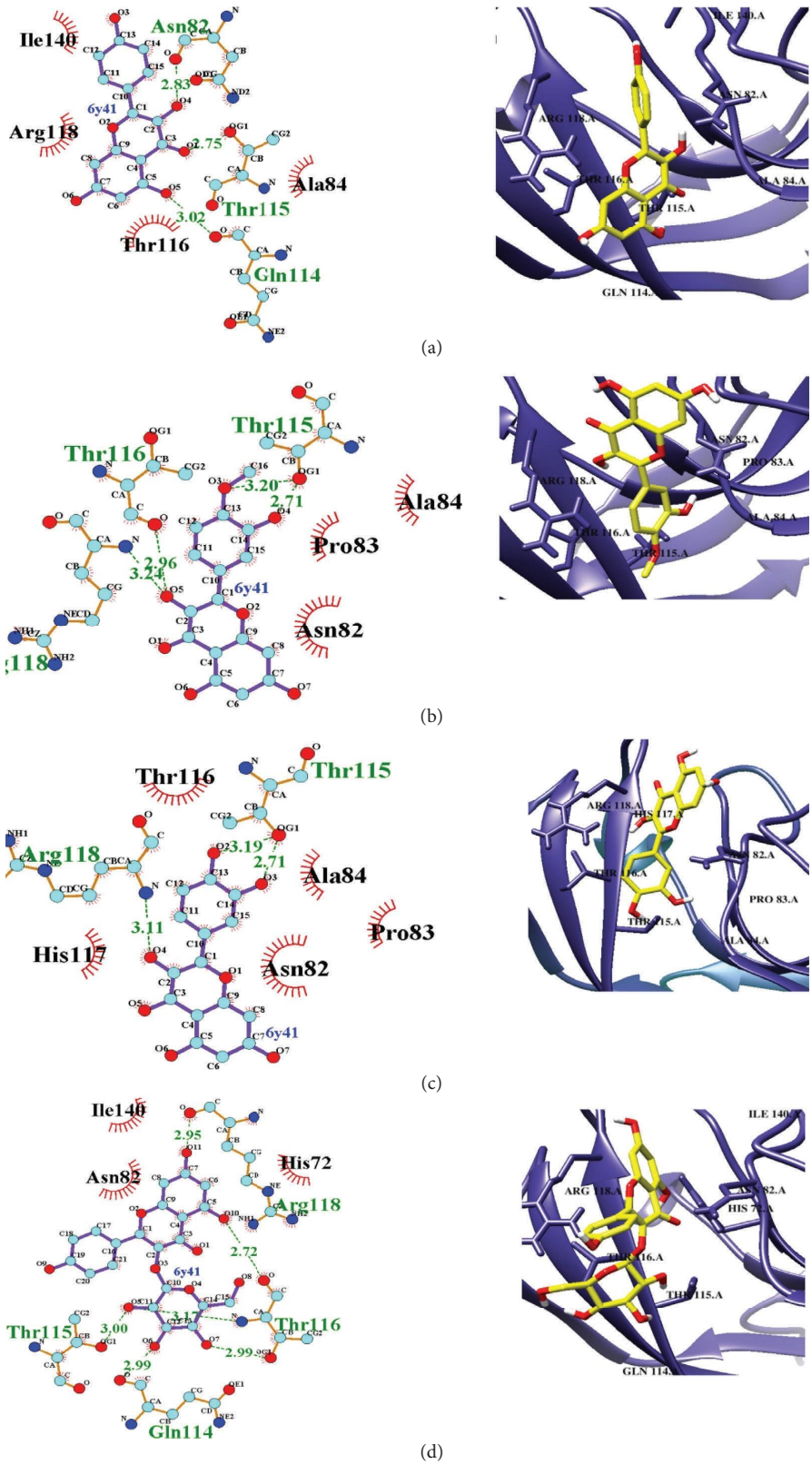

Figure 4: 2D and 3D interactions of MrpH with (a) kaempferol, (b) 4′-O-methyl quercetin, (c) quercetin, and (d) kaempferol-3-O-beta-D-glucoside.

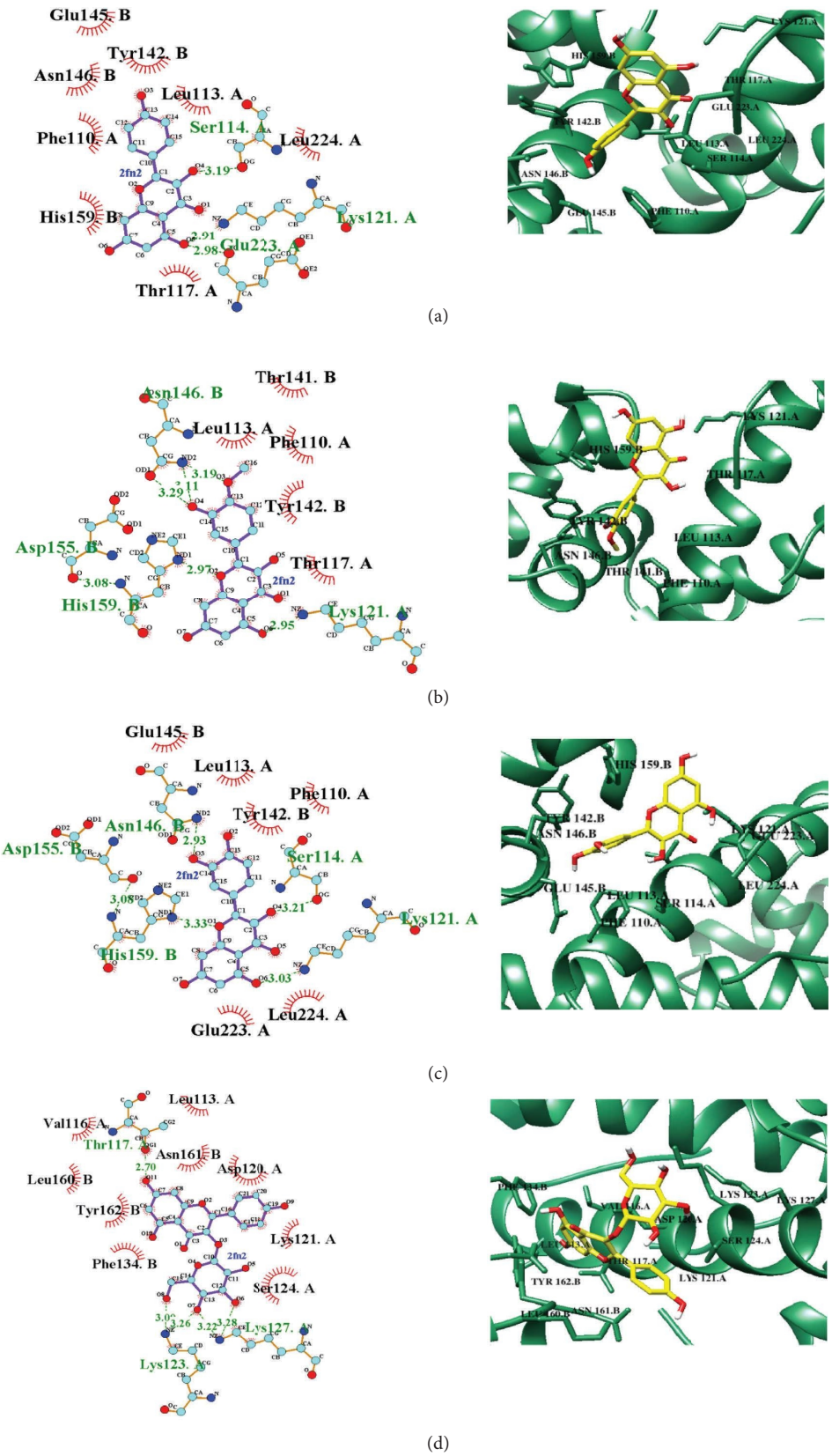

Figure 5: 2D and 3D interactions of SarA with (a) kaempferol, (b) 4′-O-methyl quercetin, (c) quercetin, and (d) kaempferol-3-O-beta-D-glucoside.

Table 2: Drug-likeness prediction by SwissADME.

Ligand	MW (g/mol)	HBA	HBD	MLOGP	TPSA (Å^2)	Drug likeness (lipinski)
Kaempferol	286.2	6	4	−0.03	111.13	Yes; zero violation
4′-O-methyl quercetin	316.3	7	4	−0.31	120.36	Yes; zero violation
Quercetin	302.2	7	5	−0.56	131.36	Yes; zero violation
K3G	448.4	11	7	−2.10	190.28	No; two violations: O or $N > 10$, OH or NH > 5

Abbreviations: HBA, number of H-bond acceptors; HBD, number of H-bond donors; K3G, kaempferol-3-O-beta-D-glucoside; MW, molecular weight; TPSA, topological polar surface area.

(Table 1) by forming three hydrogen bonds (H-bonds) with chain A. The O5 in the hydroxy function interacted through two H-bonds with Lys121 and Glu223 (bond lengths: 2.91 and 2.98 Å, respectively) (Figure 5(a)). Additionally, the O4 in the hydroxy function interacted through one H-bond with Ser114 (bond length: 3.19 Å). Moreover, several hydrophobic interactions were found, including with Thr117, Phe110, Leu113, and Leu224 (chain A) and His159, Asn146, Glu145, and Thr142 (chain B).

4′-O-methyl quercetin, with a binding affinity (BA) of −6.8 kcal/mol (Table 1), interacted through 5 hydrogen bonds (H-bonds) with the binding site of SarA. The O4 in the hydroxyl group formed two H-bonds with Asn146 in chain B (bond lengths: 3.29 and 3.11 Å) (Figure 5(b)). The O3 in the etheric part also interacted through one H-bond with this residue (bond length: 3.19 Å). Moreover, this compound created H-bonds with Lys121 (bond length: 2.95 Å; chain A) and His159 (bond length: 2.97 Å; chain B) through O6 in the hydroxy function and O2 in the etheric part. Hydrophobic interactions were formed with Thr117, Phe110, and Leu113 (chain A), and Tyr142 and Thr141 (chain B).

Quercetin showed a binding affinity of −7.4 kcal/mol (Table 1). As shown in Figure 5(c), it formed four H-bonds: O4 and O6 in the hydroxyl functions with Ser114 and Lys121 (in chain A) (bond lengths: 3.21 and 3.03 Å, respectively), and O1 and O3 in the etheric and hydroxyl functions, respectively, with His159 and Asn146 (chain B) (bond lengths: 3.33 and 2.93 Å). This compound also created hydrophobic interactions with Glu223, Leu224, Phe110, and Leu113 (chain A) and Tyr142 and Glu145 (chain B).

K3G, similar to Quercetin, exhibited a BA of −7.4 kcal/mol (Table 1) and through O11 in the hydroxy function created one H-bond with Thr117 in chain A (bond length: 2.70 Å). Hydrophobic interactions were formed with Leu113 and Lys121 in chain A and Leu160 in chain B (Figure 5(d)).

Overall, these compounds exhibited good interactions with SarA, especially quercetin, kaempferol, and 4′-O-methyl quercetin, which established significant hydrophobic interactions and H-bonds with the binding site. K3G, with a higher affinity (−7.4 kcal/mol) than kaempferol and 4′-O-methyl quercetin (−7.2 and −6.8 kcal/mol, respectively), was docked to this target protein, but the number of interactions with the key residues was lower for this compound.

Based on these results, molecular docking simulation showed that these flavonoids were stably bound to the active site of SarA and suggested their antibiofilm formation activities. Biofilms, which are surface-attached microbial communities encased in a self-produced extracellular matrix, play a critical role in the development of antibiotic resistance [32]. Consequently, targeting the formation and stability of biofilms has emerged as an alternative therapeutic strategy to conventional antibiotic treatments. Notably, studies have reported that the combined use of antibiofilm agents and antibiotics can potentiate the efficacy of antimicrobial therapy against bacterial biofilms [32].

In a similar study by Panpan and coworkers, SarA was used as a target to virtually screen natural active monomers. In that study, quercetin showed BA of −8.7 kcal/mol and through hydrophobic and hydrogen bonds [33]. In another on flavonoids, using molecular docking analysis, it was predicted that hesperidin can interact with SarA protein, which is crucial for biofilm formation [34].

3.5. ADMET Prediction. In our study, we evaluated drug similarity and likeness using Lipinski's Ro5 (Table 2). According to Ro5, compounds with a molecular weight (MW) of 500 or less, hydrogen bond acceptors (HBA) of 10 or less, hydrogen bond donors (HBDs) of 5 or less, and lipophilicity (MLOGP) of 4.15 or less are likely to have good absorption or permeation [35]. Kaempferol, quercetin, and 4′-O-methyl quercetin adhere to Ro5, while K3G violates two of these rules. We also considered the topologically polar surface area (TPSA) as a drug absorption descriptor [36].

Lower TPSA corresponds to higher membrane penetration [37]. TPSA less than 140 Å^2 indicates proper drug absorption in the intestine [38]. For kaempferol, quercetin, and 4′-O-methyl quercetin, TPSA values were in this range (< 140 Å^2). As shown in Table 3, none of these compounds can cross the blood–brain barrier (BBB). Also, they are not P-gp substrates. All compounds have high gastrointestinal (GI) absorption except K3G. In terms of CYP2C9 inhibition, only 4′-O-methyl quercetin is an inhibitor.

Toxicity prediction showed that all compounds are noncarcinogens and weak inhibitors of human ether-à-go-go-related gene (hERG). hERG channels play an essential role in cardiac action potential repolarization, and blockage

Table 3: Pharmacokinetics and toxicity prediction by SwissADME and admetSAR.

Ligand	BBB permeant	GI absorption	P-gp substrate	CYP2C9 inhibitor	Carcinogens	hERG inhibition	AMES toxicity
Kaempferol	No	High	No	No	Non-carcinogens	Weak inhibitor	Non AMES toxic
4′-O-methyl quercetin	No	High	No	Yes	Non-carcinogens	Weak inhibitor	Non AMES toxic
Quercetin	No	High	No	No	Non-carcinogens	Weak inhibitor	Non AMES toxic
Kaempferol-3-O-beta-D-glucoside	No	Low	No	No	Non-carcinogens	Weak inhibitor	AMES toxic

Abbreviations: BBB, blood–brain barrier; GI absorption, gastrointestinal absorption; hERG, human ether-ago-go-related gene; P-gp, P-glycoprotein.

of their function increases the risk of ventricular arrhythmias. Additionally, K3G was found to be AMES toxic, demonstrating this compound's mutagenicity [39]. In summary, kaempferol, quercetin, and 4′-O-methyl quercetin showed favorable ADMET properties compared to K3G.

4. Conclusion

In this study, we purified and screened four flavonoids from the flowering aerial parts of *D. semibarbatum* for their anticatheter-related bacterial effects. Notably, our docking results revealed distinct interactions: while the methoxy function in 4′-O-methyl quercetin exhibited reduced binding to the target proteins SarA and MrpH, quercetin demonstrated robust affinity with these proteins. These findings align with the observed antibiofilm activities of quercetin in our study [40]. Furthermore, considering the essential criteria for therapeutic compounds by ADMET properties and effectiveness [41], we propose that DSF, along with its major components (including quercetin and its derivatives), holds promise as a supplementary approach alongside standard antibacterial drugs. Specifically, this strategy may help mitigate the virulence of *P. mirabilis* and *S. aureus* bacteria in urinary infectious diseases [42, 43].

Data Availability Statement

The data used to support the findings of this study are available from the corresponding author upon reasonable request.

Disclosure

This work is part of the Ph.D. thesis of Dr. Mohammadreza Lotfaliani in Pharmacognosy.

Conflicts of Interest

The authors declare no conflicts of interest.

Funding

This work was supported by the Shahid Beheshti University of Medical Sciences under Grant number 12841.

References

[1] A. Mirzaei, M. Habibi, S. Bouzari, and M. R. Asadi Karam, "Characterization of Antibiotic-Susceptibility Patterns, Virulence Factor Profiles and Clonal Relatedness in Proteus Mirabilis Isolates From Patients With Urinary Tract Infection in Iran," *Infection and Drug Resistance* (2019): 3967–3979, https://doi.org/10.2147/idr.s230303.

[2] P. Y. Chung and Y. S. Toh, "Anti-Biofilm Agents: Recent Breakthrough Against Multi-Drug Resistant *Staphylococcus aureus*," *Pathogens and Disease* 70, no. 3 (2014): 231–239, https://doi.org/10.1111/2049-632x.12141.

[3] R. Wasfi, S. M. Hamed, M. A. Amer, and L. I. Fahmy, "*Proteus mirabilis* Biofilm: Development and Therapeutic Strategies," *Frontiers in Cellular and Infection Microbiology* 10 (2020): 414, https://doi.org/10.3389/fcimb.2020.00414.

[4] R. R. Muder, C. Brennen, J. D. Rihs, et al., "Isolation of *Staphylococcus aureus* From the Urinary Tract: Association of Isolation With Symptomatic Urinary Tract Infection and Subsequent Staphylococcal Bacteremia," *Clinical Infectious Diseases* 42, no. 1 (2006): 46–50, https://doi.org/10.1086/498518.

[5] B. A. Bhat, W. R. Mir, B. A. Sheikh, M. A. Rather, T. U. H. Dar, and M. A. Mir, "In Vitro And In Silico Evaluation of Antimicrobial Properties of Delphinium Cashmerianum L., A Medicinal Herb Growing in Kashmir, India," *Journal of Ethnopharmacology* 291 (2022): 115046, https://doi.org/10.1016/j.jep.2022.115046.

[6] K. Kumari, P. Adhikari, A. Pandey, S. Samant, and V. Pande, "Antimicrobial Potential of Delphinium Denudatum (Wall Ex Hook & Thom)," *Bulletin of Environment, Pharmacology and Life Sciences* 8, no. 12 (2019): 152–158.

[7] P. Asgharian, F. Heshmati Afshar, E. Mahmoodzadeh, and S. Hallaj-Nezhadi, "Antibacterial Activity of Different Extracts of Aerial Parts of *Chondrilla juncea* L, Ajuga Comata Stapf, Nepeta Ucrainica L, and Delphinium Speciosum MB," *Journal of Mazandaran University of Medical Sciences* 29, no. 180 (2019): 24–35.

[8] D.-C. Hao, P.-G. Xiao, H.-Y. Ma, Y. Peng, and C.-N. He, "Mining Chemodiversity From Biodiversity: Pharmacophylogeny of Medicinal Plants of Ranunculaceae," *Chinese Journal of Natural Medicines* 13, no. 7 (2015): 507–520, https://doi.org/10.1016/s1875-5364(15)30045-5.

[9] F. Sharifnia, M. Barani, and M. Assadi, "Notes on Some Species of the Genus Delphinium (Ranunculaceae) in Iran," *Iranian Journal of Botany* 19, no. 2 (2013): 202–210.

[10] M. Lotfaliani, M. Ghanadian, S. A. Ayatollahi, M. Aghaei, and F. Kobarfard, "Anticancer Activity of Delphinium Semibarbatum Alkaloid Fractions against LNCaP, and DU 145 Human Prostate Cancer Cells Through the Intrinsic Apoptotic Pathway," *Iranian Journal of Pharmaceutical Research: IJPR* 20, no. 4 (2021): 107–116, https://doi.org/10.22037/ijpr.2021.115462.15382.

[11] A. Mirzaei, B. Nasr Esfahani, M. Ghanadian, and S. Moghim, "Alhagi Maurorum Extract Modulates Quorum Sensing Genes and Biofilm Formation in *Proteus mirabilis*," *Scientific Reports* 12, no. 1 (2022): 13992, https://doi.org/10.1038/s41598-022-18362-x.

[12] M. B. Majnooni, S. M. Ghanadian, M. Mojarrab, et al., "Antibacterial, Antibiofilm, Antiswarming, and Antioxidant Activities of Flavonoids Isolated From Allium Colchicifolium Leaves," *Journal of Food Biochemistry* 2023 (2023): 1–14, https://doi.org/10.1155/2023/5521661.

[13] J. Przekwas, J. Gębalski, J. Kwiecińska-Piróg, et al., "The Effect of Fluoroquinolones and Antioxidans on Biofilm Formation by *Proteus mirabilis* Strains," *Annals of Clinical Microbiology and Antimicrobials* 21, no. 1 (2022): 22–10, https://doi.org/10.1186/s12941-022-00515-5.

[14] R. Durgadevi, R. Kaleeshwari, T. K. Swetha, R. Alexpandi, S. Karutha Pandian, and A. Veera Ravi, "Attenuation of *Proteus mirabilis* Colonization and Swarming Motility on Indwelling Urinary Catheter by Antibiofilm Impregnation: An In Vitro Study," *Colloids and Surfaces B: Biointerfaces* 194 (2020): 111207, https://doi.org/10.1016/j.colsurfb.2020.111207.

[15] F. Zengin, M. M. Kisla, and Z. A. Alagoz, "Molecular Docking Studies of Some Tetrahydronaphtalene-Benzimidazole Derivatives and Correlation With Their Corresponding Anti-MRSA Activities," *Journal of Faculty of Pharmacy of Ankara University* 43, no. 1 (2019): 20–27.

[16] M. A. Bratty, "Spectroscopic and Molecular Docking Studies for Characterizing Binding Mechanism and Conformational Changes of Human Serum Albumin upon Interaction With Telmisartan," *Saudi Pharmaceutical Journal* 28, no. 6 (2020): 729–736, https://doi.org/10.1016/j.jsps.2020.04.015.

[17] R. Herowati and G. P. Widodo, "Molecular Docking Studies of Chemical Constituents of Tinospora Cordifolia on Glycogen Phosphorylase," *Procedia Chemistry* 13 (2014): 63–68, https://doi.org/10.1016/j.proche.2014.12.007.

[18] A. C. Wallace, R. A. Laskowski, and J. M. Thornton, "LIGPLOT: A Program to Generate Schematic Diagrams of Protein-Ligand Interactions," *Protein Engineering Design and Selection* 8, no. 2 (1995): 127–134, https://doi.org/10.1093/protein/8.2.127.

[19] A. Daina, O. Michielin, and V. Zoete, "SwissADME: a Free Web Tool to Evaluate Pharmacokinetics, Drug-Likeness and Medicinal Chemistry Friendliness of Small Molecules," *Scientific Reports* 7, no. 1 (2017): 42717, https://doi.org/10.1038/srep42717.

[20] F. Cheng, W. Li, Y. Zhou, et al., *admetSAR: A Comprehensive Source and Free Tool for Assessment of Chemical ADMET Properties* (ACS Publications, 2012).

[21] Z. Yang, Y. Wang, Y. Wang, and Y. Zhang, "Bioassay-guided Screening and Isolation of α-Glucosidase and Tyrosinase Inhibitors from Leaves of Morus Alba," *Food Chemistry* 131, no. 2 (2012): 617–625, https://doi.org/10.1016/j.foodchem.2011.09.040.

[22] K. Yamauchi, T. Mitsunaga, M. Inagaki, and T. Suzuki, "Synthesized Quercetin Derivatives Stimulate Melanogenesis in B16 Melanoma Cells by Influencing the Expression of Melanin Biosynthesis Proteins MITF and p38 MAPK," *Bioorganic & Medicinal Chemistry* 22, no. 13 (2014): 3331–3340, https://doi.org/10.1016/j.bmc.2014.04.053.

[23] C. Yu, H. Tang, Y. Zheng, and L. Li, "Flavonoids from the Leaves of Sorbus Tianschanica," *Chemistry of Natural Compounds* 49, no. 1 (2013): 115–116, https://doi.org/10.1007/s10600-013-0524-1.

[24] Y. Xie, W. Yang, F. Tang, X. Chen, and L. Ren, "Antibacterial Activities of Flavonoids: Structure-Activity Relationship and Mechanism," *Current Medicinal Chemistry* 22, no. 1 (2014): 132–149, https://doi.org/10.2174/09298673216661409161134 43.

[25] M. He, T. Wu, S. Pan, and X. Xu, "Antimicrobial Mechanism of Flavonoids against *Escherichia coli* ATCC 25922 by Model Membrane Study," *Applied Surface Science* 305 (2014): 515–521, https://doi.org/10.1016/j.apsusc.2014.03.125.

[26] X.-M. Li, X.-G. Luo, C.-L. Si, et al., "Antibacterial Active Compounds From Hypericum Ascyron L. Induce Bacterial Cell Death through Apoptosis Pathway," *European Journal of Medicinal Chemistry* 96 (2015): 436–444, https://doi.org/10.1016/j.ejmech.2015.04.035.

[27] M. Y. Al-Nour, M. M. Ibrahim, and T. Elsaman, "Ellagic Acid, Kaempferol, and Quercetin From Acacia Nilotica: Promising Combined Drug With Multiple Mechanisms of Action," *Current pharmacology reports* 5, no. 4 (2019): 255–280, https://doi.org/10.1007/s40495-019-00181-w.

[28] G. R. Nielubowicz and H. L. Mobley, "Host–Pathogen Interactions in Urinary Tract Infection," *Nature Reviews Urology* 7, no. 8 (2010): 430–441, https://doi.org/10.1038/nrurol.2010.101.

[29] S. M. Jacobsen and M. E. Shirtliff, "*Proteus mirabilis* Biofilms and Catheter-Associated Urinary Tract Infections," *Virulence* 2, no. 5 (2011): 460–465, https://doi.org/10.4161/viru.2.5.17783.

[30] R. P. Novick, "Autoinduction and Signal Transduction in the Regulation of Staphylococcal Virulence," *Molecular Microbiology* 48, no. 6 (2003): 1429–1449, https://doi.org/10.1046/j.1365-2958.2003.03526.x.

[31] K. E. Beenken, J. S. Blevins, and M. S. Smeltzer, "Mutation of sarA in *Staphylococcus aureus* Limits Biofilm Formation," *Infection and Immunity* 71, no. 7 (2003): 4206–4211, https://doi.org/10.1128/iai.71.7.4206-4211.2003.

[32] N. Rabin, Y. Zheng, C. Opoku-Temeng, Y. Du, E. Bonsu, and H. O. Sintim, "Biofilm Formation Mechanisms and Targets for Developing Antibiofilm Agents," *Future Medicinal Chemistry* 7, no. 4 (2015): 493–512, https://doi.org/10.4155/fmc.15.6.

[33] P. Liu, X. Kang, X. Chen, X. Luo, C. Li, and G. Wang, "Quercetin Targets SarA of Methicillin-Resistant *Staphylococcus aureus* to Mitigate Biofilm Formation," *Microbiology Spectrum* 12, no. 1 (2024): e0272223–23, https://doi.org/10.1128/spectrum.02722-23.

[34] K. Vijayakumar, S. Muhilvannan, and M. Arun Vignesh, "Hesperidin Inhibits Biofilm Formation, Virulence and Staphyloxanthin Synthesis in Methicillin Resistant *Staphylococcus aureus* by Targeting SarA and CrtM: An In Vitro and In Silico Approach," *World Journal of Microbiology and Biotechnology* 38, no. 3 (2022): 44, https://doi.org/10.1007/s11274-022-03232-5.

[35] C. A. Lipinski, F. Lombardo, B. W. Dominy, and P. J. Feeney, "Experimental and Computational Approaches to Estimate Solubility and Permeability in Drug Discovery and Development Settings," *Advanced Drug Delivery Reviews* 23, no. 1-3 (1997): 3–25, https://doi.org/10.1016/s0169-409x(96)00423-1.

[36] C. Xu and X. Chen, "Molecular Property–Affinity Relationship of the Interaction Between Dietary Polyphenols and Bovine Milk Proteins," *Food & Function* 2, no. 7 (2011): 368–372, https://doi.org/10.1039/c1fo10074b.

[37] A. Fulp, K. Bortoff, Y. Zhang, H. Seltzman, R. Snyder, and R. Maitra, "Towards Rational Design of Cannabinoid Receptor 1 (CB1) Antagonists for Peripheral Selectivity," *Bioorganic & Medicinal Chemistry Letters* 21, no. 19 (2011): 5711–5714, https://doi.org/10.1016/j.bmcl.2011.08.032.

[38] G. Prasanthi, "In-silico Estimation on Oral Bioavailability and Drug-Likeness of Mono and Bis-Mannich Bases of Piperazine Derivatives," *Journal of Global Trends in Pharmaceutical Sciences* 5 (2014): 1485–1488.

[39] M. H. A. Al-Jumaili, F. Siddique, F. Abul Qais, et al., "Analysis and Prediction Pathways of Natural Products and Their Cytotoxicity against HeLa Cell Line Protein Using Docking, Molecular Dynamics and ADMET," *Journal of Biomolecular Structure and Dynamics* 41, no. 3 (2023): 765–777, https://doi.org/10.1080/07391102.2021.2011785.

[40] X. He, W. Zhang, Q. Cao, et al., "Global Downregulation of Penicillin Resistance and Biofilm Formation by MRSA Is Associated with the Interaction Between Kaempferol Rhamnosides and Quercetin," *Microbiology Spectrum* 10, no. 6 (2022): e2822, https://doi.org/10.1128/spectrum.02782-22.

[41] N. Hussain, B. B. Kakoti, M. Rudrapal, et al., "Bioactive Antidiabetic Flavonoids From the Stem Bark of *Cordia dichotoma* Forst: Identification, Docking and ADMET Studies," *Molbank* 2021, no. 2 (2021): M1234, https://doi.org/10.3390/m1234.

[42] P. Chemmugil, P. Lakshmi, and A. Annamalai, "Exploring Morin as an Anti-Quorum Sensing Agent (Anti-QSA) Against Resistant Strains of *Staphylococcus aureus*," *Microbial Pathogenesis* 127 (2019): 304–315, https://doi.org/10.1016/j.micpath.2018.12.007.

[43] V. Gopu, C. K. Meena, and P. H. Shetty, "Quercetin Influences Quorum Sensing in Food Borne Bacteria: In-Vitro and In-Silico Evidence," *PLoS One* 10, no. 8 (2015): e0134684, https://doi.org/10.1371/journal.pone.0134684.